

Exploring the Affinity and Interactions of Piperine with Wild-Type and Mutated *PTEN* through Molecular Docking and Dynamics Simulations

Abdul Satar Bahadorpor¹, Abdullah Sahar², Abdul Musawer Bayan¹, Rafiullah Shirzadi¹, *Sayed Hussain Amiri³

1. Medical Sciences Research Center, Ghalib University, Kabul, Afghanistan

2. Department of Microbiology, Faculty of Medical Laboratory Technology, Spinghar Institute of Higher Education, Kabul, Afghanistan

3. Curative Medicine, Khatam-Al-Nabieen University, Kabul, Afghanistan

ARTICLE INFO

Type: Original Article

Received: 02 September, 2024

Accepted: 18 December, 2024

*Corresponding Author:

E-mail: amirihussain706@gmail.com

To cite this article: Bahadorpor AS, Sahar A, Bayan AM, Shirzadi A, Amiri SH. Exploring the Affinity and Interactions of Piperine with Wild-Type and Mutated *PTEN* through Molecular Docking and Dynamics Simulations.

Afghanistan Journal of Basic Medical Sciences. 2025 Jan 2(1):64-80.

<https://doi.org/10.62134/khatamuni.70>

ABSTRACT

Background: *Phosphatase and tensin homolog (PTEN)* gene dysfunction plays an essential role in the pathogenesis of cancer development. Piperine is a natural compound, popularized by its effective medicinal properties. In this investigation, we used in-silico techniques such as molecular docking and molecular dynamic simulation to assess the activating effect of piperine on *PTEN* which can guide the development of more personalized therapeutic strategies or to provide more effective therapies and interventions.

Methods: The analysis was performed in Ghalib Bioinformatics Center, Kabul, Afghanistan in 2024. For molecular docking purposes, autodock 4.2.2 was applied to determine the interaction and binding affinity of Piperine with both Wild-type and Mutated-type *PTEN*. For molecular dynamics (MD) simulation purposes AMBER99SB force field within GROMACS 2019.6 software was utilized to find more molecular interaction and structural conformations.

Results: Wild and mutated-type *PTENs* had favorable interaction and binding energy, with -6.99 (kcal/mol) for Wild-type *PTEN* and -6.35 (kcal/mol) for Mutated-type *PTEN*. The result of the MD simulation showed the stabilization and less fluctuation of wild-type *PTEN* in the presence of piperine.

Conclusion: This study provides the details that piperine with its multi-health benefits and usage, could be likely as a potential activator for wild-type *PTEN*, offering valuable insights in generating new treatments to fight against cancers and reduce its development risk.

Keywords: Wild-type *PTEN*, Mutated *PTEN*, Piperine, Molecular docking, Molecular dynamics simulation

Introduction

It was anticipated that 20 million new cases of cancer were diagnosed worldwide in 2022. In line with the patterns of aging and population growth, this number shows a

constant rise from prior years (1). A projected 10 million deaths worldwide were attributed to cancer in 2022, making it one of the major causes of death globally, accounting for

around one in six fatalities (1). Cancer of lung is the leading cause of cancer death globally, responsible for around 1.8 million total cancer deaths (2). Cancer is a group of diseases characterized by the uncontrolled proliferation and spread of abnormal cells throughout the body (3). Normally, cells grow, divide, and die in a controlled manner; however, in cancer, this process is disrupted, and cells begin to grow uncontrollably (4). Cancer is caused by a variety of factors, including genetics, environmental exposures (such as tobacco smoke, radiation, or chemicals), infections (such as HPV), and lifestyle choices (5).

The symptoms and treatment options differ greatly depending on the type of cancer, but common treatments include surgery, chemotherapy, radiation therapy, immunotherapy, and targeted therapy (6). To prevent the development of cancer, tumor suppressor genes are crucial in controlling cell growth and proliferation (7). These genes produce peptides that regulate DNA repair and act as a cell cycle braking system when DNA damage occurs. The normal control mechanisms that interrupt excessive cell proliferation are lost when these genes are mutated or inactivated, which aids in the development and spread of tumors (8).

The most well-known tumor suppressor genes are *APC*, *RBI*, *BRCA1*, *TP53*, *PTEN*, and *BRCA2* (9). *Phosphatase and Tensin Homolog*, or *PTEN*, is an essential tumor suppressor gene that controls several biological functions, such as migration, autophagy, growth and survival (10).

PTEN mainly functions by inhibiting the PI3K/AKT pathway, a signaling cascade involved in cell survival and growth (10). Under normal conditions, when growth factors activate PI3K, the enzyme produces PIP3, which activates AKT, promoting cell proliferation and survival. *PTEN* counteracts this by dephosphorylating PIP3 back to PIP2, thereby inhibiting AKT activation and

preventing uncontrolled cell growth. This makes *PTEN* essential for maintaining the balance between cell proliferation and apoptosis. In addition to regulating the PI3K/AKT pathway, *PTEN* also controls the cell cycle and apoptosis. It helps regulate key proteins that ensure proper cell cycle progression and promotes apoptosis in response to DNA damage, preventing the survival of abnormal or damaged cells (11). Furthermore, *PTEN* influences cell processes that are important for tissue development and repair but can contribute to cancer metastasis if uncontrolled (12). When *PTEN* is mutated or lost, as commonly seen in various cancers, its ability to regulate these processes is compromised, leading to excessive cell proliferation, evasion of apoptosis, and increased migration and invasion, all of which contribute to cancer development (13). Thus, *PTEN* acts as a critical tumor suppressor, maintaining cellular homeostasis and preventing the growth and spread of tumors (14). The loss of *PTEN* function, often through mutations or deletions, is a significant driver of cancer progression in multiple tissue types, including breast, prostate, endometrial, and brain tumors (15-18). *PTEN* mutations not only contribute to tumor growth but also to the ability of cancer cells to spread and form secondary tumors (19). Research performed on *PTEN* with in-silico technique usage shows the effect of natural components such as Thymoquinone analogs and Naringin on this tumor suppressor gene (20). Additionally, other researches unveils the reactivation of *PTEN* by dCas9-VPR, synthetic transcription factors and Substances present in cruciferous (21).

Piperine, which is an active alkaloid found in black pepper (*Piper nigrum*) has molecular formula of C₁₇H₁₉NO₃ and its structure consists of a piperidine ring linked to a trans-cinnamoyl group via an amide bond (22). The compound features both aromatic and

heterocyclic functional groups, contributing to its biological activity. Piperine is lipophilic, meaning it dissolves easily in fats and organic solvents, but it has low solubility in water (23). This lipophilic characteristic plays a key role in its ability to cross biological membranes, influencing its absorption and bioavailability.

Piperine had a wide range of pharmacological benefits. One of its most notable properties is its ability to enhance the bioavailability of nutrients and drugs by inhibiting key drug-metabolizing enzymes, such as cytochrome P450 (24), and modulating intestinal absorption by affecting membrane transporters (25). This makes piperine an effective bioenhancer, often combined with other compounds like curcumin to improve therapeutic efficacy (26). Piperine also exhibits potent anti-inflammatory and antioxidant effects, helping to reduce oxidative stress and inflammation in the body (27). It has shown anticancer potential by inducing apoptosis, suppressing tumor cell growth, and inhibiting angiogenesis (28, 29). Additionally, piperine offers neuroprotective benefits, including memory enhancement and protective effects against neurodegenerative diseases such as Alzheimer and Parkinsonism (30, 31). Its antimicrobial properties further expand its therapeutic applications, making piperine a valuable compound in both traditional medicine and modern drug development.

By utilizing molecular docking and molecular dynamics (MD) simulation studies, we aimed to find the molecular interaction of wild *PTEN* and mutated *PTEN* by particular mutations (Val119Ile (V119I), Val158Ile (V158I), and Arg234Gln (R234Q) with Piperine (32). In addition, recent research performed using molecular techniques showed the favorable interactions and potential activating effects of curcumin on wild *PTEN* (33). By performing this study, we wanted to shed light on the piperine effect

in the structural and interactional alteration of wild-type *PTEN* and its mutated forms *PTEN* which offers an innovative approach to deal with cancers.

Materials and Methods

Enzymes and Piperine Structure Selection

The research performed in Ghalib Bioinformatics Center, Kabul, Afghanistan in 2024. The tertiary structures of *PTEN* with 2.1Å resolution were obtained from the RCSB Protein Data Bank (PDB ID: 1D5R)(34). The additional water molecules and co-crystal ligands were removed from the 1D5R pdb file to make it ready for use of AutoDock software and the Amber forcefield. V119I, V158I, and R234Q mutation points were established on wild-type *PTEN* pdb file by utilizing VMD software. The structure of Piperine, with CID 638024 code, was downloaded from the Pubchem database and optimized by using Openbabel software (converting sdf format to pdb) (35).

Molecular Docking (MD)

MD utilized to determine the interactions, binding affinity and constant inhibition between wild *PTEN* and Mutated *PTEN* with Piperine. For docking purpose, autodock 4.2.2 software was applied. After removal of water molecules and co-crystal ligands from the download pdb files, the enzyme structures were introduced for energy minimization by optimizing the GROMACS 2019.6 package with the AMBER99SB force field (36). The binding sites of the enzymes were determined as Gly165, Lys164, Thr167, Ile168, Val166, Asp326, Pro169, and Asn329, in which previously reported. Grid box selected with 60×60×60 dimensions' points and with grid point spacing of 0.375 Å. Following it, 200 docking calculations with 25 million energy evaluations by employing Lamarckian genetic algorithm (LGA), were executed. The best docking conformation with the lowest

binding energy in highly populated cluster was chosen for the molecular dynamics' simulation.

Molecular Dynamics Simulation

MD simulations were used to study the wild *PTEN* and Mutated *PETN* interaction with Piperine in detailed pattern by using the GROMACS 2019.6 program and the AMBER99SB force field. After preparation of topology files, ions such as chloride (Cl^-) and Sodium (Na^+) added to maintain neutralizations of complexes and then the simulations were performed in a cubic box solvated by water. ACPYPE tool was applied to obtain the necessary parameters for Piperine. After it, systems equilibrated at 1 ns simulation in the NVT and NPT ensembles at 310 K and 1 bar. Following the system equilibration, MD simulation with 200 ns was conducted, utilizing a time step of 2 femtoseconds (fs). MD simulations trajectories were used in reporting analysis such as RMSD, RMSF, RG, SASA and H-bond interaction between Piperine and Enzymes, Enzyme-Enzyme and Enzyme-Solvent.

Results

Molecular docking

The obtained docking parameters such as binding energies and inhibition constants of Piperine with the wild and mutated *PTEN*, exhibited in Table 1. Accordingly, Piperine maintain proper affinity for wild and mutated *PTEN*s. In addition, the wild type *PTEN* complex manifesting the lowest binding energy compared to mutated type *PTEN*. Figure 1 depicted the binding pose of Piperine within the binding sites of Wild-type and Mutated-type *PTEN* enzymes.

Figure 1a exhibiting the van der Waals interactions of Piperine with the amino acids Val166, Thr167, Pro169, Arg172, Arg173, Tyr176, Asn320, Asp,324 and Lys332 of Wild-type *PTEN*. This plot describing that the hydroxyl group of Piperine formed a hydrogen bond with carbonyl group of Lys332. In addition, Figure 1b depicts the hydrogen bonding of Piperine with active site's residues of Mutated-type *PTEN* Pro169, Arg172, Tyr176, Tyr177, Leu30 and Asn323. The hydroxyl group of Piperine formed hydrogen bond with carboxyl group of Arg172.

Table 1: The obtained docking features predicted by AutoDock program.

<i>Complex</i>	<i>Wild-type PTEN/ Piperine</i>	<i>Mutated PTEN/ Piperine</i>
Cluster rank	3	1
Number in cluster	167	39
Lowest Binding Energy (kcal/mol)	-6.99	-6.35
$K_i(\mu\text{M})$	22.11	7.47

Molecular dynamic simulation

By completion of MD computation, we optimized MD simulation calculation to find out the structural stability and residual variation of complexes, mainly to certify the output parameters of MD. Molecular dynamic simulation results were utilized to investigate the interactions and structural changes of piperine with both wild and mutated *PTEN*.

The analysis plot of the MD simulation parameter includes RMSD, RMSF, RG, SASA and the H-bond analysis of protein-ligand, protein-protein and protein solvent. These analyses are initial for understanding the activity of enzymes in presence of piperine and in their free form.

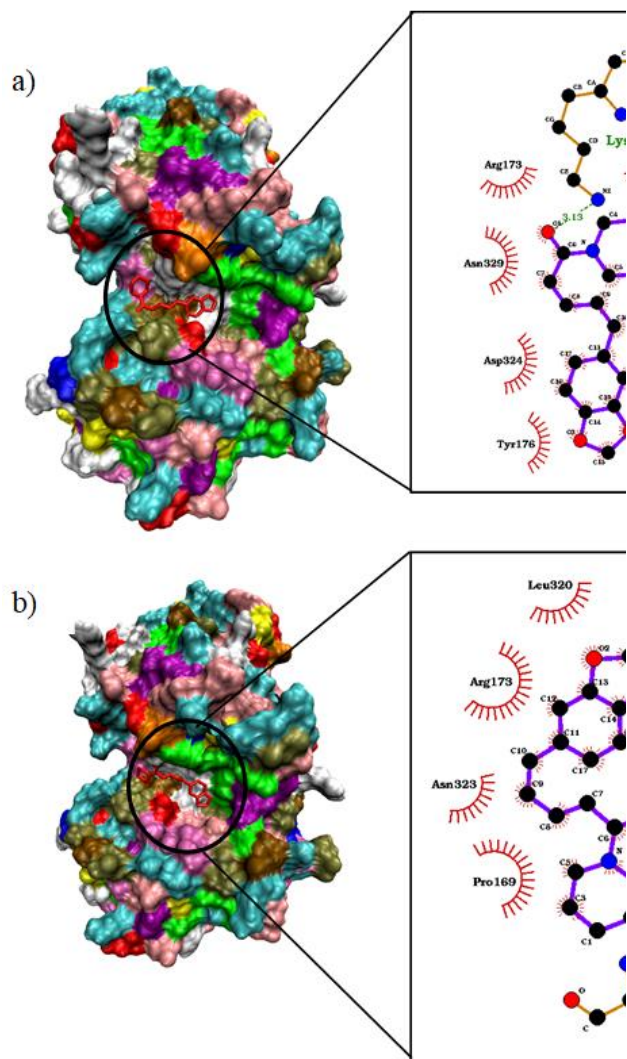


Figure 1: The best suitable docking pose and molecular interactions of the Piperine with wild type and Mutated type *PTEN* respectively. Figures provided by VMD1.9.3 and Ligplot+ programs.

Structural analysis

With performing RMSD analysis, we can find out the conformational changes and stability of complexes during simulation time boundary. Figure 2 illustrating the RMSD of free enzymes and complexed with Piperine. According to Figure 2a, both free wild and free mutated *PTEN* reached equilibrium at 160ns. As depicted in Figure 2b, Wild type *PTEN* undergoes less structural fluctuation in presence of Piperine, compared with free Wild type *PTEN*. In Figure 2c, the Free Mutated *PTEN* has more structural instability rather than its complex form. Free mutated

PTEN reached in equilibrium approximately in 140 ns but in presence of Piperine the system reaches in 180ns. Comparing fig 2b and 2c, wild type *PTEN* in presence of piperine has more structural stability rather than Mutated-*PTEN*/Piperine complexes. Piperine could disrupt the structure and function of Mutated *PTEN*. The average and standard deviations of RMSD presented in Table 2. In this table, binding of Piperine decreased the average RMSD of wild-type from 0.261 ± 0.018 ns to 0.214 ± 0.015 ns respectively but binding of piperine to Mutated-type *PTEN* raised up the average

RMSD from 0.263 ± 0.0271 ns to 0.285 ± 0.033 ns, it means Wild-type *PTEN* well equilibrated in presence of piperine, in which

it means Piperine has this potential activating role on wild-type *PTEN*.

Table 2: The average and standard deviations of RMSD, Rg, RMSF and SASA for free and complex enzymes during the last 30ns.

System	Mean RMSD (nm)	Mean Rg (nm)	Mean RMSF (nm)	Mean SASA (nm ²)
Free Wild-type <i>PTEN</i>	0.261 ± 0.018	2.196 ± 0.007	0.183 ± 0.079	170.006 ± 1.524
Wild-type <i>PTEN</i> / Piperine	0.214 ± 0.015	2.209 ± 0.008	0.130 ± 0.068	161.944 ± 1.482
Free mutated <i>PTEN</i>	0.263 ± 0.0271	2.227 ± 0.010	0.180 ± 0.071	165.350 ± 1.680
Mutated <i>PTEN</i> / Piperine	0.285 ± 0.033	2.222 ± 0.010	0.134 ± 0.061	166.803 ± 1.605

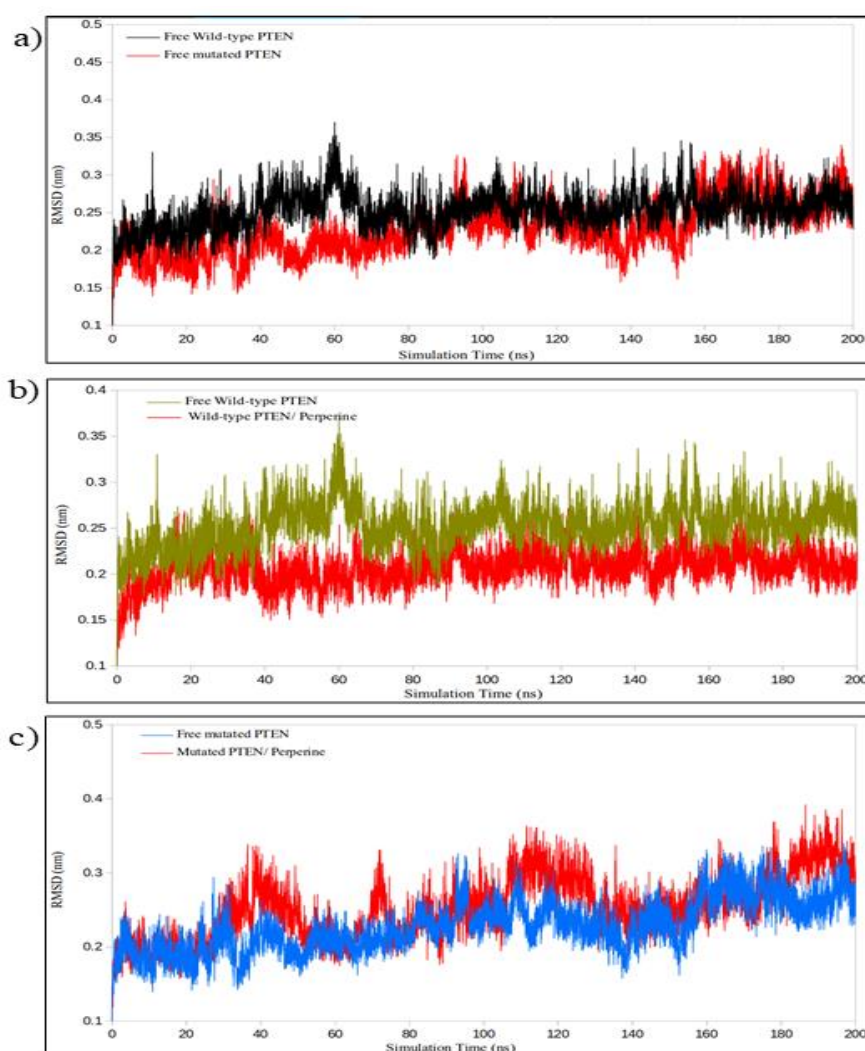


Figure 2: RMSD plots of free and bound enzymes for a) Free Wild and Mutated *PTEN*, b) Wild-type *PTEN* and c) Mutated-type *PTEN*.

In order to find the structural compactness and structural variation of Protein-Ligand Rg

analysis is necessary to be measured. The RG for both systems are presented in Figure 3. In

Figure 3b, Wild-type *PTEN* undergoes structural compression in presence of Piperine. Oppositely the binding of Piperine to Mutated-type *PTEN* minimize its structural compactness. In Table 2, average RG value for free Wild-type *PTEN* 2.196 ± 0.007 ns increased to 2.209 ± 0.008 ns

in presence of Piperine. In which binding of Piperine to Mutated *PTEN* showing a decline in average RG value from 2.227 ± 0.010 ns to 2.222 ± 0.010 ns respectively. Verifying above interpretation about RG graphic representation.

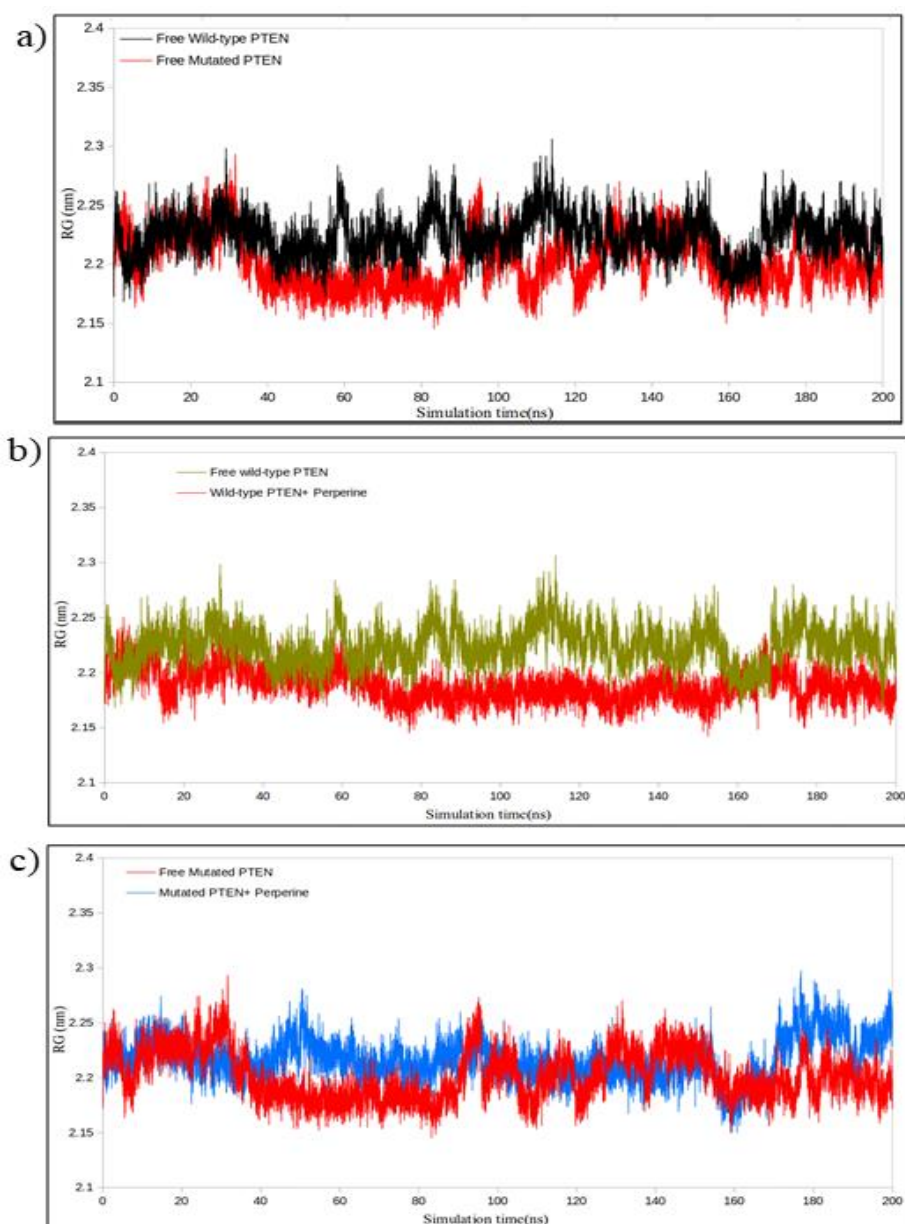


Figure 3: RG plots of free and bound enzymes for a) Free Wild and Mutated *PTEN*, b) Wild-type *PTEN* and c) Mutated-type *PTEN*.

The RMSF measurement help us to understand the residue deviation and

fluctuation of free and complex systems. RMSF values for all free and complex

systems displayed in Figure 4. Analysis of Figure 4a showing that the free wild-type *PTEN* has less fluctuation in residue level rather than Mutated-type *PTEN*. Based on the Figure 4a, the complex form of Piperine with Wild-type *PTEN*, highly minimize its fluctuation in residue site rather than free Wild-type *PTEN*. The same scenario also occurred with Mutated-type *PTEN* in

presence of Piperine. As represented in Table 2, RMSF value of Wild-type *PTEN* decreased in presence of Piperine from 0.183 ± 0.079 ns to 0.130 ± 0.068 ns, also for Mutated-type *PTEN* from 0.180 ± 0.071 ns to 0.134 ± 0.061 ns in presence of Piperine respectively. The residue are stabilizes in both systems in presence of Piperine.

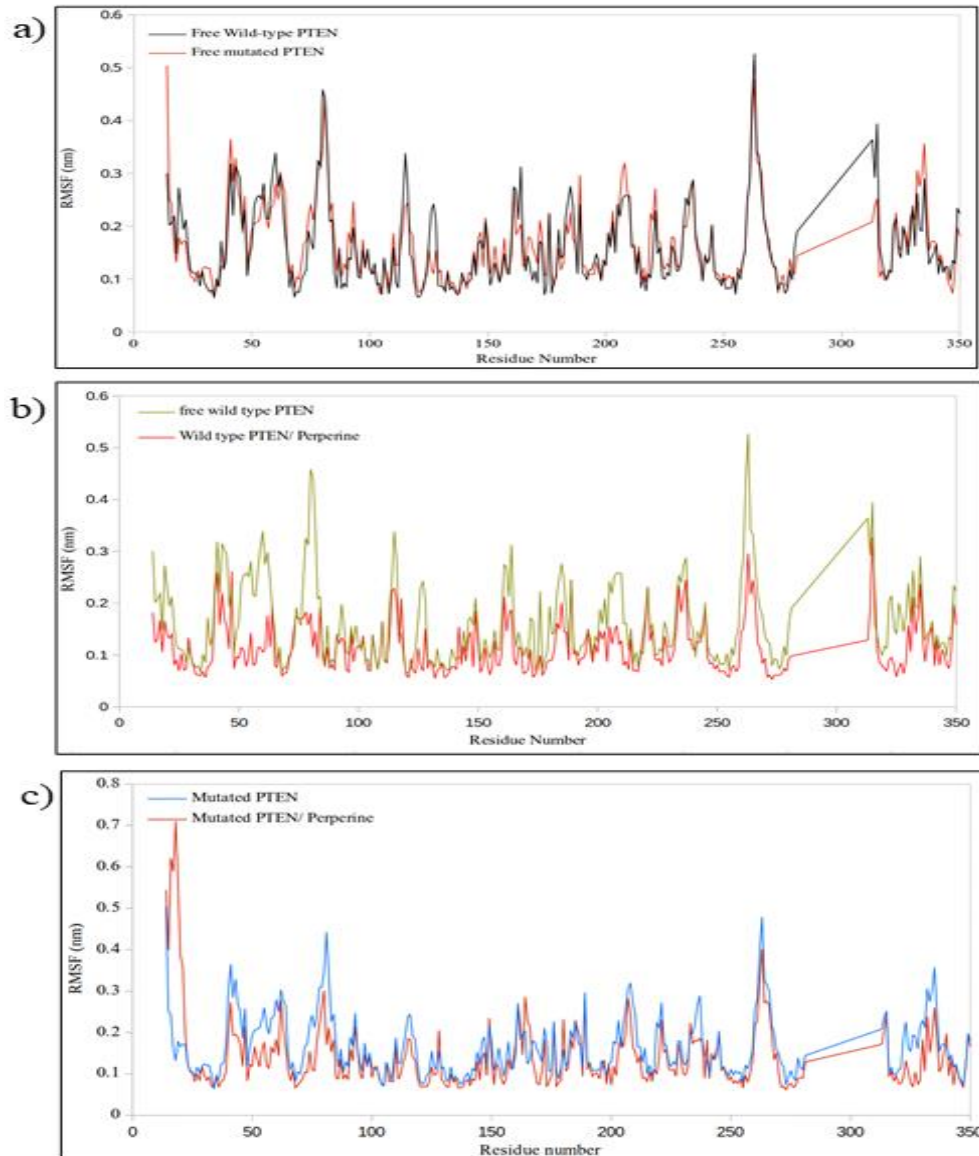


Figure 4: RMSF plots of free and bound enzymes for a) Free Wild and Mutated *PTEN*, b) Wild-type *PTEN* and c) Mutated-type *PTEN*.

SASA analysis is an essential tool for obtaining knowledge about biomolecule

surface area accessible to solvent, in which it is important for understanding molecular

interactions during the simulation time boundary. Figure 5 depicts the SASA plot for Wild and Mutated PTEN. Figure 5a illustrating the average of SASA for the Free mutated-type PTEN, was declined in contrast with free Wild-type PTEN. According to Figure 5b, the SASA plot for Wild-type

PTEN had decreased in presence of Piperine but there is an increased in SASA plot of Mutated *PTEN* in presence of Piperine, indicating that the accessible surface area of Wild-type *PTEN* for water molecules is decreased, due to replacement of the existed solvent in active site of this protein.

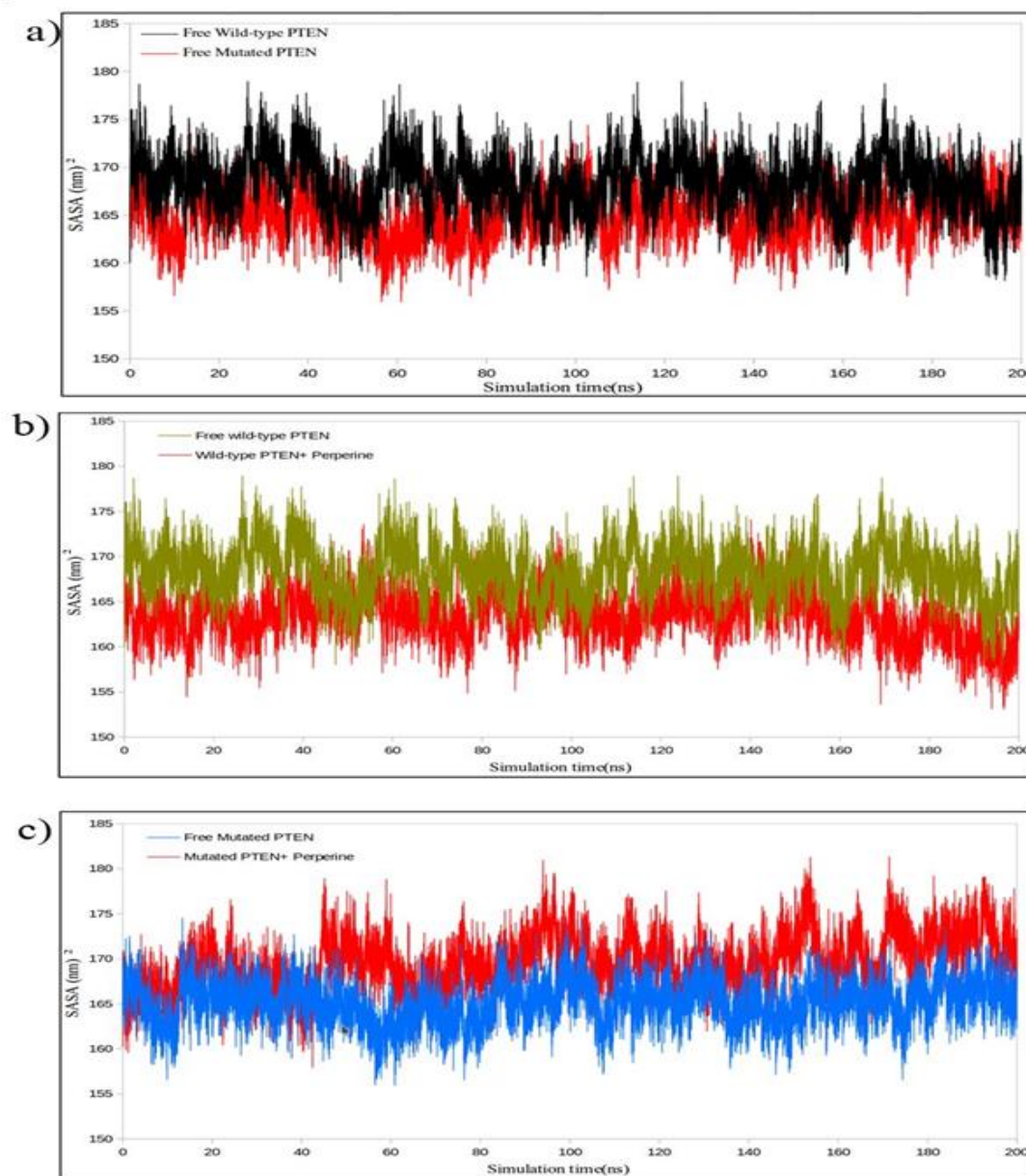


Figure 5: SASA plots of free and bound enzymes for a) Free Wild and Mutated PTEN, b) Wild-type *PTEN* and c) Mutated-type *PTEN*.

In Table 2, the average SASA value for wild-type *PTEN* has decreased when Piperine

binds to it from 170.006 ± 1.524 ns to 161.944 ± 1.482 ns. Additionally, there is an

increase in average SASA value for Mutated-type *PTEN* from 165.350 ± 1.680 ns to 166.803 ± 1.605 ns. Some part of this protein opened and exposure to water molecules. Furthermore, the reduction in the average solvent-accessible surface area (SASA) for wild type *PTEN* in presence piperine is attributed to an increase in structural compactness, as evidenced by the decreased radius of gyration (Rg). The enhanced compactness of the enzyme's structure in the presence of piperine results in a smaller surface area exposed to solvents, limiting accessibility. The increase in SASA for

mutated *PTEN* in presence of piperine could be due to opening and uncompressing of mutated *PTEN* structure, thereby the average number Rg for mutated *PTEN* increased in presence of piperine.

To gain a detailed understanding of ligand behavior during molecular dynamics simulations, a snapshot analysis was carried out to examine the positional alterations of Piperine within the both *PTEN*'s active site over 200 ns. Snapshots were taken at 50 ns intervals, as depicted in Figure 6, providing insight into the interaction dynamics.

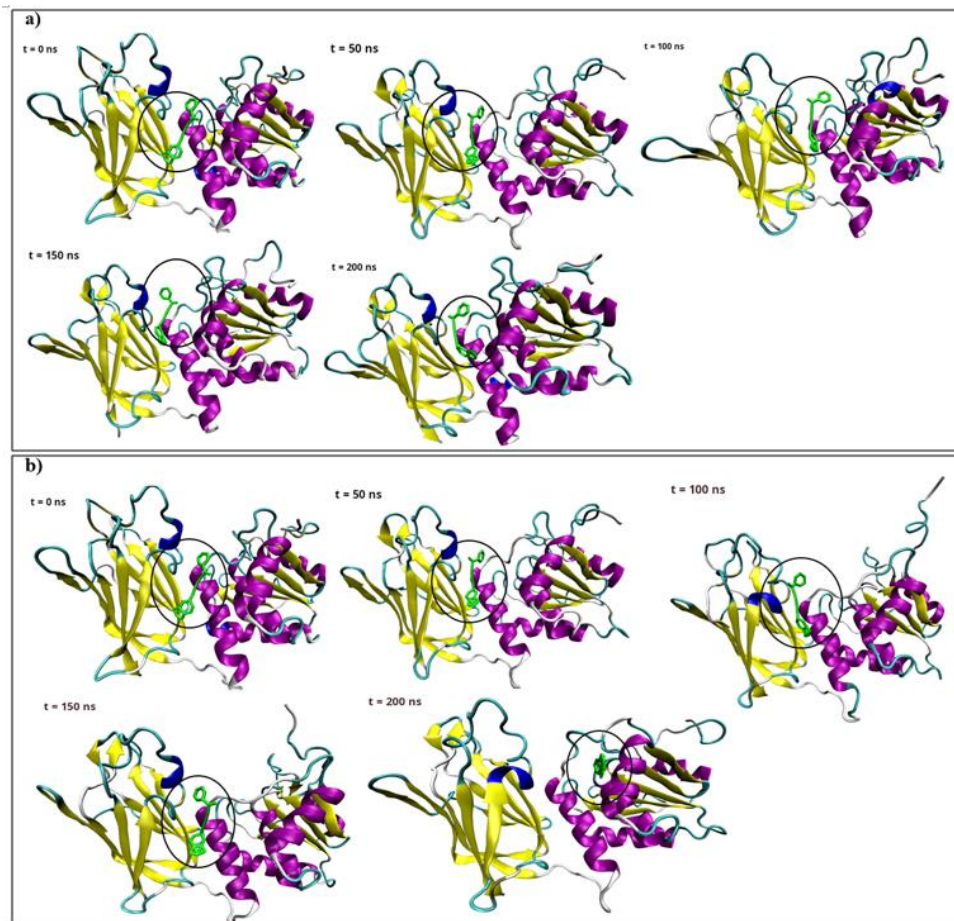


Figure 6: Snapshots plots of the a) Wild type *PTEN*/Piperine complex, b) Mutated type *PTEN*/Piperine complex generated by VMD software.

Piperine remained consistently localized within the active site throughout the simulation for wild type PTEN, without migrating to other regions of the enzyme surface. This stability is a strong indicator of its specific binding affinity. However, Piperine underwent more major conformational shifts within the active site of Mutated-type PTEN. In addition, this plot transferring this idea that the piperine with its less conformational and locational changes within the active site of wild-type PTEN, could potentially be a good indicator for activating the Wild-type PTENs.

Interactions Analysis

Analyzing hydrogen bonding between enzymes and ligands is important for finding the stability of their complexes and molecular interactions. The Figure 7 depicts the number of hydrogen bonds formed between Piperine and the wild and mutated *PTEN* during a 200 ns simulation time. Piperine formed up to two hydrogen bonds with Wild-type and Mutated-type *PTEN* respectively, highlighting the stability of these complexes. Figures 8 and 9 displaying the hydrogen bond counts between enzyme-enzyme and enzyme-solvent interactions for both free and complexes during the simulation. Table 3 summarizes the average hydrogen bond counts for these interactions during the last 30 ns of the simulation. In the presence of Piperine, the Wild-type *PTEN* enzyme showed an increase in average hydrogen bonds from 220.512 ± 7.409 ns to 227.837 ± 8.475 ns. Moreover, there is an increase in average number of enzyme-enzyme hydrogen bond of Mutated-type *PTEN* in presence of Piperine from 222.105 ± 8.081 ns to 225.917 ± 8.040 ns respectively. possibly due to changes in its

secondary structure. The average enzyme-solvent hydrogen for both Wild and Mutated type *PTEN* had been diminished in presence piperine, due to replacing the hydrogen bond between solvent and enzymes with the piperine hydrogen bond. SASA analysis, as previously explained, also demonstrated a reduction for wild type *PTEN* in the presence of piperine, further supporting the assertion of piperine increases intermolecular interactions and decreases the enzyme's solvent-accessible surface area. This highlights its role in altering the enzyme's structural exposure to the surrounding environment. The same scenario also occurred for mutated type *PTEN* respectively.

Analysis of the molecular mechanics Poisson-Boltzmann surface area method (MMPBSA)

The MMPBSA method was employed to evaluate the binding energy components, such as van der Waals, electrostatic, polar solvation, and SASA energies, using trajectory data from the final 30 ns to validate the results of the docking studies. Similar to the docking predictions, the binding free energy calculations using the MMPBSA method confirmed the stability of Wild-type PTEN/Piperine complex. The summarized findings, displayed in Table 4, indicated that piperine established favorable interactions with Wild-type PTEN/Piperine complex, with the strongest binding affinity. This stability was evident from the negative net binding free energy values, with the Wild-type PTEN/Piperine complex displaying values of -139.897 ± 14.711 (kJ/mol). For the Mutated-type PTEN/Piperine complex, the net binding free energy was calculated as -135.260 ± 17.892 (kJ/mol).

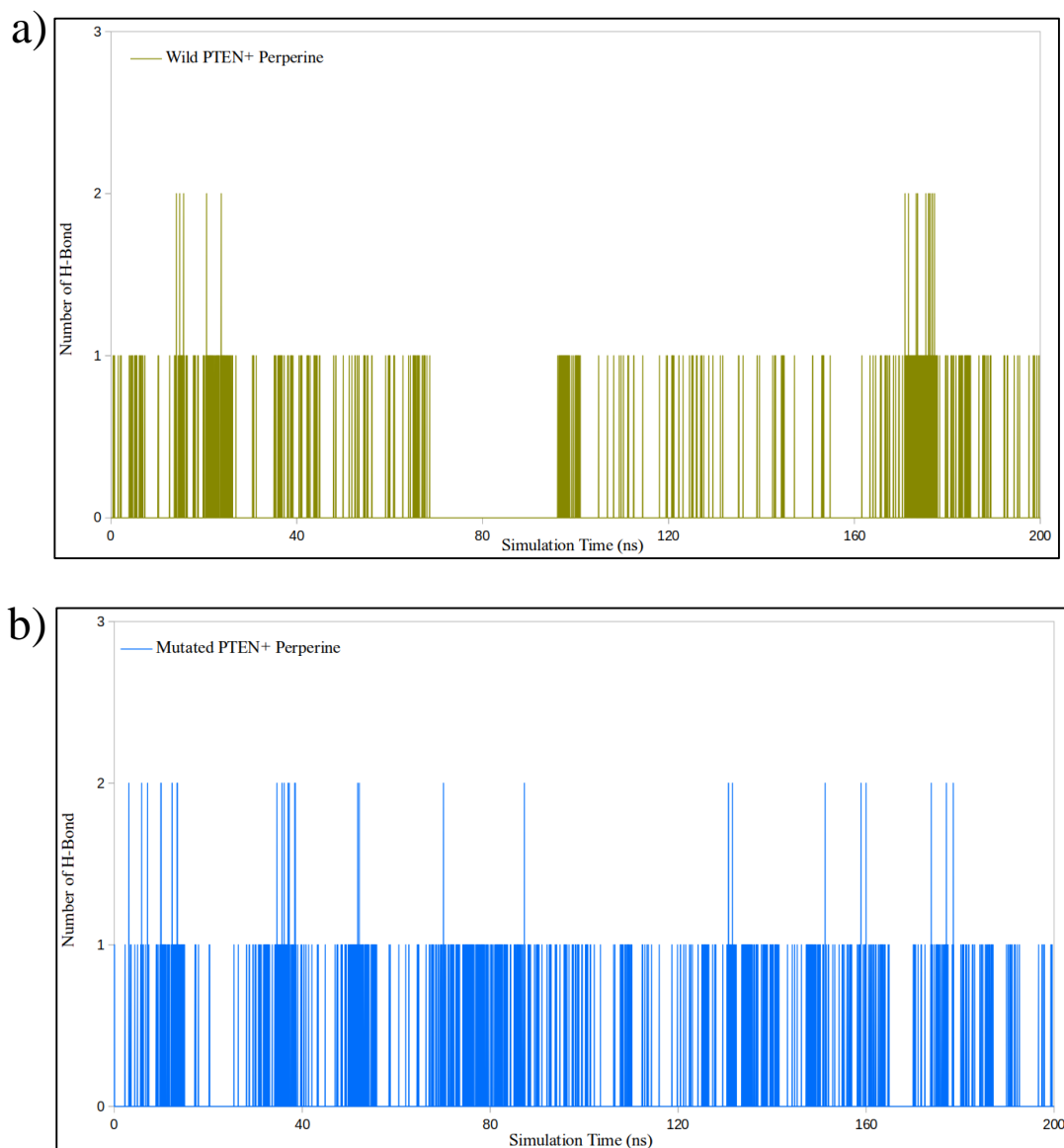


Figure 7: Time dependence of the number of hydrogen bonds between Piperine and enzymes for a) Wild-type *PTEN* and b) Mutated-type *PTEN* during the simulation time.

Table 3: The average and standard deviations of intra molecular enzyme and enzyme-solvent hydrogen bonds during last 30 ns.

<i>System</i>	<i>Enzyme-Enzyme</i>	<i>Enzyme-Solvent</i>
Free Wild-type <i>PTEN</i>	220.512 ± 7.409	667.404 ± 16.579
Wild-type <i>PTEN</i> / Piperine	227.837 ± 8.475	647.613 ± 17.126
Free mutated <i>PTEN</i>	222.105 ± 8.081	667.422 ± 16.442
Mutated <i>PTEN</i> / Piperine	225.917 ± 8.040	659.217 ± 15.959

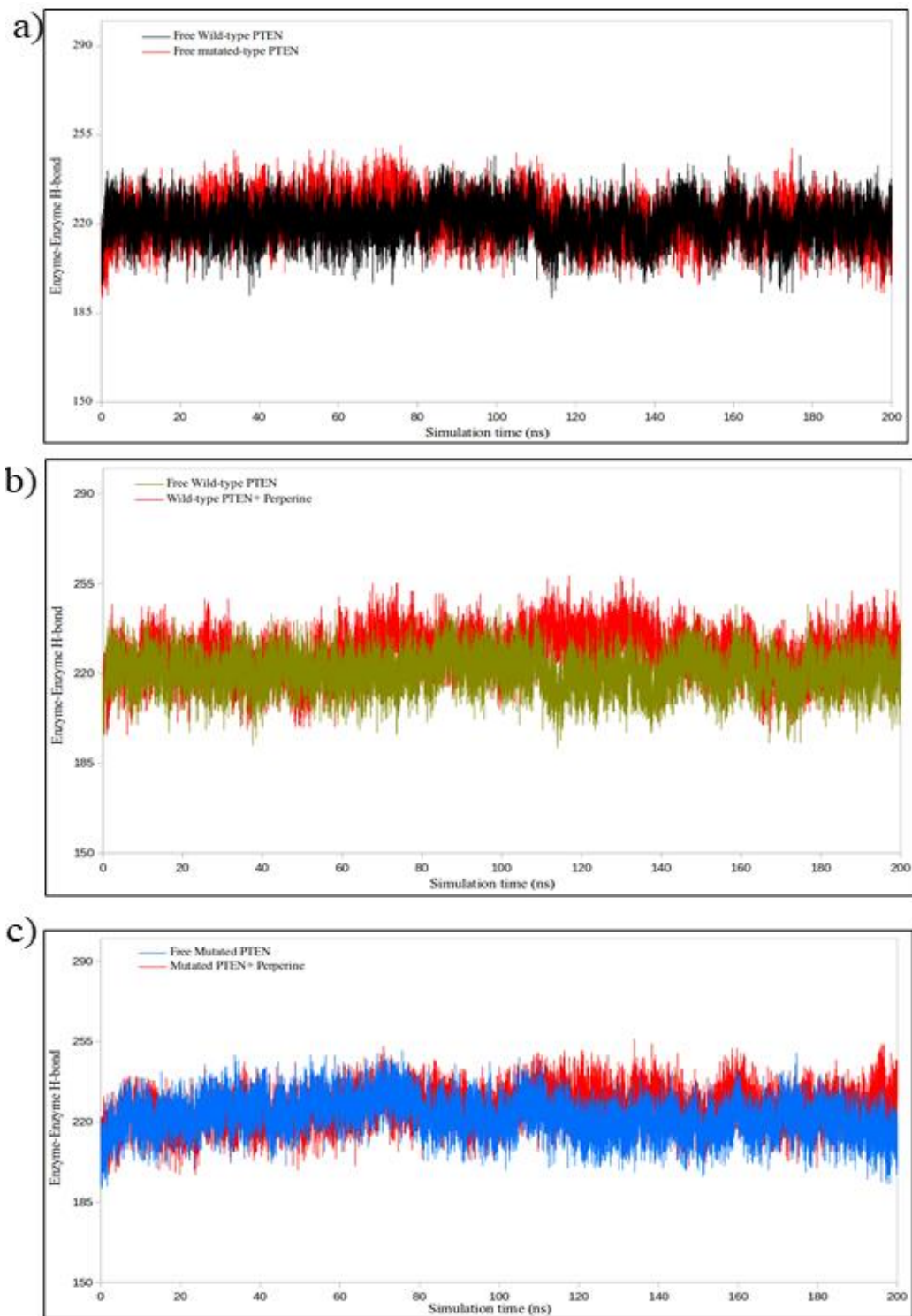


Figure 8: Enzyme-Enzyme H-bond plots of free and bound enzymes for a) Free PTENs, b) Wild-type *PTEN* and c) Mutated-type *PTEN*.

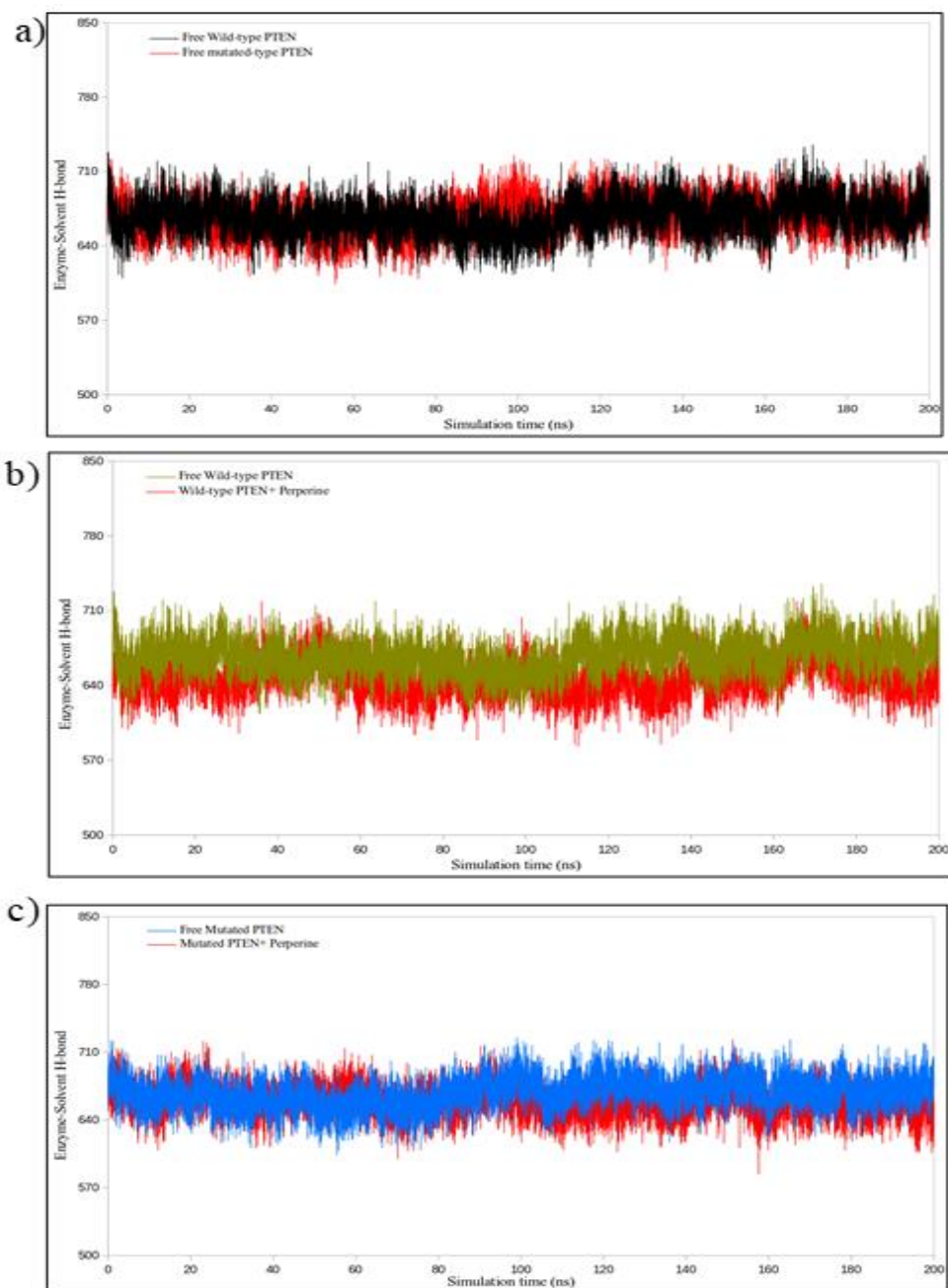


Figure 9: Enzyme-Solvent H-bond plots of free and bound enzymes for a) Free PTENs, b) Wild-type *PTEN* and c) Mutated-type *PTEN*.

Table 4: The average of energy components for complexes analysed by MMPBSA.

<i>Energy components (kJ/mol)</i>	<i>Wild-type PTEN/ Piperine</i>	<i>Mutated PTEN/ Piperine</i>
van der Waal energy	-187.427±12.257	-188.985±13.872
Electrostatic energy	-4.792 ±4.925	-4.001 ± 4.464
Polar solvation energy	66.398 ±10.894	69.638±13.810
SASA energy	-13.077± 0.874	-12.912±1.075
Binding energy	-139.897±14.711	-135.260±17.892

Discussion

This study applied molecular docking in 200 population size and molecular dynamics simulations with 200 ns simulation time to explore the activating role of Piperine on PTEN.

The results of this study suggest that piperine could serve as a potential activator of wild type *PTEN* through its lowest binding energy and high affinity. Recent research performed on studying the effect of curcumin on wild type and mutated type *PTEN* utilizing molecular docking and MD simulation unveiled that curcumin effectively interacted with mutated *PTEN* compared to wild type *PTEN*, which could serve as an inhibitor of Mutated type *PTEN* (33). However, the result of our study showed the promising activation of wild type *PTEN* by piperine.

Various studies have employed computational approaches to examine the impact of natural compounds, such as Thymoquinone analogs and Naringin, on *PTEN*, as documented in this research articles, as results of their study revealed that the *PTEN* has good molecular interactions, binding stability with Naringin and with up-regulating the expression of *PTEN* gen by Thymoquinone (20, 37). *PTEN* reactivation can be accomplished using compounds derived from cruciferous vegetables and synthetic transcription factors like dCas9-VPR (21, 38).

Conclusion

The docking analysis showed that Piperine interacted favorably with both *PTEN*, forming hydrogen bonds and van der Waals interactions. RMSD analysis revealed that Piperine stabilized the structures of Wild-type *PTEN*, while destabilizing Mutated-type *PTEN*. The radius of gyration plots indicated structural compression of Wild-type *PTEN*

structures, but expansion in Mutated-type *PTEN*. RMSF analysis unveiled a decrease for both Wild and Mutated *PTEN* in presence of Piperine. Moreover, SASA analysis showed up a decrease in Wild-type *PTEN* but an increase in Mutated-type *PTEN*. The hydrogen bonds analysis between Piperine and the enzymes show the stability of complexes throughout the simulation time. By analyzing the molecular interaction of Piperine with Wild-type *PTEN* and Mutated-type *PTEN*, we understand this that piperine has potentially more activating effect on Wild-type *PTEN* by stabilizing its structural integrity, maintaining its functionality. The result of this study could be helpful in generating this natural component as precursor for treatment of cancers associated with *PTEN*s dysfunction, in which could be effective for reducing mortality rate due to these fatal diseases, however to prove this more in-vitro and in-vivo experiments are required.

Acknowledgments

This research was supported by resources supplied by the deputy of financial affairs of the Ghalib University, Kabul, Afghanistan. The authors would like to express their utmost gratitude to the Board of Directors of Ghalib University, Kabul, Afghanistan for support and motivations, especially Dr. M. I. Noori, Eng. A. Ahadi and Mr. N. A Nadeem. Special thanks to Mr. Mohammad Yousoof Saleh (Head of HR and financial affairs of Ghalib University) and his team, for assisting us in better performance of this study.

Conflict of interest

The authors declare that there is no conflict of interests.

References

1. Bray F, Laversanne M, Sung H, Ferlay J, Siegel RL, Soerjomataram I, et al. Global cancer statistics 2022: GLOBOCAN estimates of incidence and mortality worldwide for 36 cancers in 185 countries. *CA Cancer J Clin.* 2024;74(3):229-63.
2. Zhou J, Xu Y, Liu J, Feng L, Yu J, Chen D. Global burden of lung cancer in 2022 and projections to 2050: Incidence and mortality estimates from GLOBOCAN. *Cancer Epidemiol.* 2024;93:102693.
3. Weinberg RA. How cancer arises. *Sci Am.* 1996;275(3):62-70.
4. Pantel K, Alix-Panabieres C, Riethdorf S. Cancer micrometastases. *Nat Rev Clin Oncol.* 2009;6(6):339-51.
5. Feinberg AP, editor *The epigenetics of cancer etiology.* Semin Cancer Biol. ; 2004: Elsevier.
6. Padma VV. An overview of targeted cancer therapy. *Biomedicines.* 2015;5:1-6.
7. Marshall CJ. Tumor suppressor genes. *Cell.* 1991;64(2):313-26.
8. Macleod K. Tumor suppressor genes. *Curr Opin Genet Dev.* 2000;10(1):81-93.
9. Joyce C, Rayi A, Kasi A. Tumor-suppressor genes. PMID: 30335276 Bookshelf ID: NBK532243. 2018.
10. Dahia P. PTEN, a unique tumor suppressor gene. *Endocr Relat Cancer.* 2000;7(2):115-29.
11. Liu A, Zhu Y, Chen W, Merlino G, Yu Y. *PTEN* dual lipid-and protein-phosphatase function in tumor progression. *Cancers.* 2022;14(15):3666.
12. Peglion F, Capuana L, Perfettini I, Boucontet L, Braithwaite B, Colucci-Guyon E, et al. *PTEN* inhibits AMPK to control collective migration. *Nat Commun.* 2022;13(1):4528.
13. Fedorova O, Parfenyev S, Daks A, Shuvalov O, Barlev NA. The Role of *PTEN* in Epithelial–Mesenchymal Transition. *Cancers.* 2022;14(15):3786.
14. Hopkins BD, Hodakoski C, Barrows D, Mense SM, Parsons RE. *PTEN* function: the long and the short of it. *Trends Biochem Sci.* 2014;39(4):183-90.
15. Haas-Kogan D, Stokoe D. *PTEN* in brain tumors. *Expert Rev Neurother.* 2008;8(4):599-610.
16. Li S, Shen Y, Wang M, Yang J, Lv M, Li P, et al. Loss of *PTEN* expression in breast cancer: association with clinicopathological characteristics and prognosis. *Oncotarget.* 2017;8(19):32043.
17. Jamaspishvili T, Berman DM, Ross AE, Scher HI, De Marzo AM, Squire JA, et al. Clinical implications of *PTEN* loss in prostate cancer. *Nat Rev Urol.* 2018;15(4):222-34.
18. Djordjevic B, Hennessy BT, Li J, Barkoh BA, Luthra R, Mills GB, et al. Clinical assessment of *PTEN* loss in endometrial carcinoma: immunohistochemistry outperforms gene sequencing. *Mod Pathol.* 2012;25(5):699-708.
19. Bazzichetto C, Conciatori F, Pallocca M, Falcone I, Fanciulli M, Cognetti F, et al. *PTEN* as a prognostic/predictive biomarker in cancer: an unfulfilled promise? *Cancers.* 2019;11(4):435.
20. Hokmabady L, Fani N. In silico elucidation of the interactions of thymoquinone analogues with phosphatase and tensin homolog (*PTEN*). *J Mol Model.* 2022;28(10):321.
21. Moses C, Nugent F, Waryah CB, Garcia-Bloj B, Harvey AR, Blancafort P. Activating *PTEN* tumor suppressor expression with the CRISPR/dCas9 system. *Mol Ther Nucleic Acids.* 2019;14:287-300.
22. Qu H, Lv M, Xu H. Piperine: Bioactivities and structural modifications. *Mini Rev Med Chem.* 2015;15(2):145-56.
23. Salsabila H, Fitriani L, Zaini E. Recent strategies for improving solubility and oral bioavailability of piperine. *Int J Appl Pharm.* 2021;13(4):31-9.
24. Pradeepa B, Vijayakumar T, Manikandan K, Kammala AK. Cytochrome P450-mediated alterations in clinical pharmacokinetic parameters of conventional drugs coadministered with piperine: a systematic review and meta-analysis. *J Herb Med.* 2023;41:100713.
25. Han H-K. The effects of black pepper on the intestinal absorption and hepatic metabolism of drugs. *Expert Opin Drug Metab Toxicol.* 2011;7(6):721-9.

26. Suresh D, Srinivasan K. Studies on the in vitro absorption of spice principles—curcumin, capsaicin and piperine in rat intestines. *Food Chem Toxicol.* 2007;45(8):1437-42.
27. Chung HY. Anti-inflammatory and antioxidant activities of piperine on t. BHP-induced Ac2F cells. *J. Food Sci. Technol.* 2019.
28. Doucette CD, Hilchie AL, Liwski R, Hoskin DW. Piperine, a dietary phytochemical, inhibits angiogenesis. *J Nutr Biochem.* 2013;24(1):231-9.
29. Manayi A, Nabavi SM, Setzer WN, Jafari S. Piperine as a potential anti-cancer agent: a review on preclinical studies. *Curr Med Chem.* 2018;25(37):4918-28.
30. Bi Y, Qu P-C, Wang Q-S, Zheng L, Liu H-L, Luo R, et al. Neuroprotective effects of alkaloids from *Piper longum* in a MPTP-induced mouse model of Parkinson's disease. *Pharm Biol.* 2015;53(10):1516-24.
31. Obulesu M, Jhansilakshmi M. Neuroprotective role of nanoparticles against Alzheimer's disease. *Curr Drug Metab.* 2016;17(2):142-9.
32. Lumb CN, Sansom MS. Defining the membrane-associated state of the *PTEN* tumor suppressor protein. *Biophys J.* 2013;104(3):613-21.
33. Malekzada MF, Mosawi SH, Fani N, Nazir S. Integrating molecular docking and molecular dynamics simulation approaches for investigation of the affinity and interactions of the Curcumin with phosphatase and tensin homolog (*PTEN*) and mutated *PTEN*. *J Mol Struct.* 2024;1318:139306.
34. Berman HM, Westbrook J, Feng Z, Gilliland G, Bhat TN, Weissig H, et al. The protein data bank. *Nucleic Acids Res.* 2000;28(1):235-42.
35. Morris GM, Goodsell DS, Halliday RS, Huey R, Hart WE, Belew RK, et al. Automated docking using a Lamarckian genetic algorithm and an empirical binding free energy function. *J Comput Chem.* 1998;19(14):1639-62.
36. Van Der Spoel D, Lindahl E, Hess B, Groenhof G, Mark AE, Berendsen HJ. GROMACS: fast, flexible, and free. *J Comput Chem.* 2005;26(16):1701-18.
37. Muthumanickam S, Indhumathi T, Boomi P, Balajee R, Jeyakanthan J, Anand K, et al. In silico approach of naringin as potent phosphatase and tensin homolog (*PTEN*) protein agonist against prostate cancer. *J Biomol Struct Dyn.* 2022;40(4):1629-38.
38. Lee Y-R, Chen M, Lee JD, Zhang J, Lin S-Y, Fu T-M, et al. Reactivation of *PTEN* tumor suppressor for cancer treatment through inhibition of a *MYC-WWP1* inhibitory pathway. *Science.* 2019;364(6441):eaau0159.